HHS Public Access

Author manuscript

J Neuroimmune Pharmacol. Author manuscript; available in PMC 2019 June 11.

Published in final edited form as:

J Neuroimmune Pharmacol. 2016 March ; 11(1): 61–72. doi:10.1007/s11481-015-9627-8.

ABCA1 is Necessary for Bexarotene-Mediated Clearance of Soluble Amyloid Beta from the Hippocampus of APP/PS1 Mice

Angela W. Corona[1], **Nathan Kodoma**[1], **Brad T. Casali**[1], and **Gary E. Landreth**[1]

[1]Department of Neurosciences School of Medicine, Case Western Reserve University, 2210 Circle Dr., Rm E649, Cleveland, OH 44106-4928, USA

Abstract

Alzheimer's disease (AD) is characterized by impaired clearance of amyloid beta (Aβ) peptides, leading to the accumulation of Aβ in the brain and subsequent neurodegeneration and cognitive impairment. ApoE plays a critical role in the proteolytic degradation of soluble forms of Aβ. This effect is dependent upon lipidation of ApoE by ABCA1-mediated transfer of phospholipids and cholesterol. ApoE and ABCA1 are induced by the action of the RXR agonist, bexarotene. We have previously shown that bexarotene reduces Aβ levels in AD mouse models and we have hypothesized that this effect requires ABCA1-mediated lipidation of ApoE. To test this hypothesis, we crossed ABCA1-deficient (ABCA1 KO) mice with the APP/PS1 model of AD. Aged ABCA1 WT and ABCA1 KO APP/PS1 mice were treated for 7 days with vehicle or bexarotene (100 mg/kg/day). Bexarotene reduced levels of soluble Aβ 1–40 and 1–42 in the hippocampus of ABCA1 WT but not ABCA1 KO APP/PS1 mice. In contrast, insoluble levels of Aβ, and plaque loads were unaffected by bexarotene in this study. ABCA1 KO mice had increased levels of inflammation compared with ABCA1 WT mice. Bexarotene also increased most inflammatory gene markers evaluated. The effect of bexarotene on microglial inflammatory profiles, however, was independent of ABCA1 genotype. Importantly, bexarotene ameliorated deficits in novel object recognition in ABCA1 WT but not ABCA1 KO APP/PS1 mice. These data indicate that ABCA1-induced lipidation of ApoE is necessary for the ability of bexarotene to clear hippocampal soluble Aβ and ameliorate cognitive deficits.

Keywords

ABCA1; ApoE; Alzheimer's disease; Microglia; Bexarotene; Amyloid beta

Introduction

Alzheimer's disease (AD) is characterized by impaired clearance of amyloid beta (Aβ) from the brain, leading to the accumulation of Aβ and subsequent deposition of Aβ plaques, hyperphosphorylation of tau, and neuronal death (Wildsmith et al. 2013). In non-diseased

Correspondence to: Gary E. Landreth.

Conflict of Interest G.E.L. is a co-founder of Rexceptor, Inc., a bio-technology company developing RXR agonists for the treatment of neurodegenerative diseases. All other authors declare no conflicts of interest.

Ethical Approval All applicable international, national, and/or institutional guidelines for the care and use of animals were followed.

human brains, the rate of production and clearance of Aβ are 7.6 % and 8.3 %, respectively (Bateman et al. 2006). Thus, even minor deficits in Aβ clearance will lead to accumulation and deposition. Notably, the strongest genetic risk factor for AD is apolipoprotein E (APOE) genotype, with the Apoε4 allele conferring an increased risk of AD (Verghese et al. 2011). Furthermore, the rate of clearance of Aβ is dependent on the apoE isoform, with the half-life of Aβ in the brain of aged AD mice being drastically increased by possession of a human ApoE4 allele (Castellano et al. 2011). These findings implicate cholesterol metabolism and transport as being integral to the pathophysiology of AD.

ATP-binding cassette A1 (ABCA1) is a six-transmembrane protein that shuttles lipids and cholesterol onto lipid-free apolipoproteins, which act as a scaffold for the formation of HDL particles. Apolipoprotein A1 (ApoA1) is the main lipoprotein in the periphery, while ApoE is the principal lipoprotein in the brain. ABCA1 is necessary for the creation of HDL particles, as genetic deletion of ABCA1 nearly abolishes lipidiation of apoliproteins throughout the body (Hirsch-Reinshagen et al. 2004). Thus, ABCA1 is the essential step for reverse cholesterol transport in the body. This is relevant because we, and others, have identified lipidated ApoE as an essential mediator of proteolytic degradation of soluble forms of Aβ in the context of AD (Cramer et al. 2012; Donkin et al. 2010; Jiang et al. 2008). Furthermore, genetic inactivation of ABCA1 resulted in increased levels of soluble and insoluble Aβ and increased plaque pathology in various mouse models of AD (Hirsch-Reinshagen et al. 2005; Koldamova et al. 2005; Wahrle et al. 2005). In contrast, genetic overexpression of ABCA1 caused a pronounced reduction in levels of soluble Aβ and plaques (Wahrle et al. 2008). These data strongly point to ABCA1-mediated lipidation of ApoE being necessary for the efficient clearance of Aβ from the brain.

ABCA1 is transcriptionally regulated by nuclear receptors -Liver X receptors (LXRs) and Peroxisome Proliferator-activated gamma receptors (PPARγs) (Koldamova et al. 2010). These receptors act as lipid sensors to regulate reverse cholesterol transport. LXRs and PPARγs form obligate heterodimers with Retinoic X Receptors (RXRs), thus, both LXRs and PPARγs will be activated by agonists of RXR. Nuclear receptors have been identified as potential therapeutic targets in AD. Indeed, agonists of nuclear receptors have been shown to reduce Aβ pathology and improve cognition in mouse models of AD (Skerrett et al. 2014). Importantly, functional ABCA1 was necessary for the LXR agonist, GW3965, to reduce Aβ pathology and reverse deficits in novel object recognition (Donkin et al. 2010). However, it is possible that nuclear receptor agonists may work through additional mechanisms, such as altering the inflammatory status of microglia (Zelcer et al. 2007).

We have previously shown that bexarotene, an FDA approved RXR agonist, was effective in reducing levels of Aβ and improving cognitive ability in the APP/PS1 mouse model of amyloidosis (Cramer et al. 2012). In the present study, we test the hypothesis that ABCA1 is necessary for the action of bexarotene. We show that ABCA1 is necessary for bexarotene-mediated clearance of soluble Aβ from the hippocampus of APP/PS1 mice and for improved cognition in novel object recognition. We also show that bexarotene induces inflammatory changes that are independent of ABCA1 genotype.

Methods

Experimental Design and Animal Model

APP/PS1Δe9 (APP/PS1) mice on a C57Bl/6 background from Jackson Labs were used. APP/PS1 mice express human APP under the prion promoter with the Swedish (K670M/N671L) mutations and the human PS1 gene deleted for exon 9 (Jankowsky et al. 2001). ABCA1 null (KO) mice on a DBA background were crossed with APP/PS1 mice to generate ABCA1 wild-type (WT) and ABCA1 KO APP/PS1 mice. All mice that were used were on a mixed C57Bl/6/ DBA background. Unless otherwise specified, ABCA1 WT and ABCA1 KO refer to these genotypes crossed with APP/PS1 mice. In addition, ABCA1 KO and ABCA1 WT nontransgenic controls (i.e., not containing human APP and PS1 genes; ABCA1 KO/nt and ABCA1 WT/nt), were included as behavioral controls and baseline inflammation controls. To complete the study, 4 separate age-matched cohorts of female mice were evaluated to yield an n of at least 10–12 for each group. Mice were treated for 7 days with vehicle (water) or bexarotene (Targretin™, Valaent Pharmaceuticals), and the contents of the capsule was dispersed in water to maintain microcrystalline drug formulation at 100 mg/kg/day then administered by oral gavage. In the last days of treatment, mice were evaluated for cognitive performance in the open field test (OFT) and novel object recognition test (NOR; day 5), and contextual fear conditioning (CFC; days 6 and 7). Following drug treatment and behavioral testing on day 7, mice were sacrificed and the brain was removed. The left hemisphere of the brain was fixed and processed for immunohisotochemistry, and the right hemisphere of the brain was dissected separately into the hippocampus (HP) and cortex (CX).

Western Blotting

CX or HP samples were mechanically dissociated in tissue homogenization buffer (THB; 2 mM Tris pH 7.4, 250 mM sucrose, 0.5 mM EDTA, 0.5 mM EGTA) containing 1:100 dilution of protease inhibitor cocktail (Roche). Homogenate was centrifuged and clarified lysates were aliquoted, flash frozen on dry ice, and stored at −80 °C until further analysis. Samples were diluted with 3× Laemmli's buffer containing 1:20 1 M DTT and boiled for 1 min to denature samples. Total protein was determined by BCA assay, and an equal amount of protein was loaded onto a precast 4–12 % bis-tris plus polyacrylamide gel (Novex) and separated at 90 V for 1.5 h.

Native gel electrophoresis was performed to determine the amount of lipidated ApoE (Cramer et al. 2012). Protein samples were prepared as described above except protein lysate was used fresh immediately following homogenization, mixed with non-denaturing sample buffer, and loaded onto a precast 4–20 % tris-glycine gel (Novex) and separated at 90 V for 3 h. A high molecular weight standard (GE High Molecular Weight Native Marker Kit 17044501) was included to differentiate lipidated vs unlipidated ApoE. Lipidated ApoE was considered to be species that were larger than 8.0 nm.

Separated proteins on gel were transferred to nitrocellulose membranes which were blocked in 5 % non-fat dry milk in PBS-T and probed with antibodies for ABCA1, ABCG1, ApoE, and β-actin (catalog numbers and company). Western blots were developed using

appropriate goat or rabbit HRP-labeled secondary antibodies and a chemiluminescent substrate kit. Densitometry was performed using ImageJ and results are expressed as relative percent of the control group.

ELISA

ELISA analysis for soluble and insoluble Aβ 1–40 and 1–42 was performed as described previously (Jiang et al. 2008). Briefly, brain homogenate from the CX or HP was processed by serial extractions in buffer containing 0.4 % diethyamine (DEA) followed by formic acid (FA), to extract the soluble and insoluble protein fractions, respectively. DEA or FA samples were diluted in ELISA buffer containing 0.05 % Tween-20 and 1 % BSA. Diluted samples were loaded onto ELISA plates coated with 6E10 antibody (Biolegend) to capture Aβ peptides. Human amyloid beta 1–40 or 1–42 was loaded to determine a standard curve. Aβ was detected using an HRP labelled antibody for either Aβ 1–40 or 1–42 (Biolegend). ELISA was developed using TMB substrate and stopped with 1 N HCL. Plates were read at 450 nm and concentrations of Aβ in sample were determined using the standard curve. Values are expressed as a relative % of the control group (ABCA1 WT/ APP/PS1 mice treated with vehicle).

Immunohistochemistry

One hemisphere of the brain was immersion-fixed in 4 % PFA in 0.1 M Phosphate buffer (PB) for at least 24 h followed by cryoprotection in a sequential gradient of 10, 15, and 30 % sucrose in PBS for at least 24 h. Brains were then flash frozen in dry-ice-cooled isopentane. Brains were mounted with O.C.T. compound (Sakura Finetek USA, Inc.) and sectioned on a cryostat. Free-floating 25 μm brain sections were collected sequentially in a 24-well plate in cryoprotection buffer (30 % glycerol, 30 % ethylene glycol, in 0.1 M phosphate buffer) and stored at −20 °C until staining.

Every 6th section through the hippocampus was stained with antibodies for Aβ (6E10; Covance) and Iba1 (Wako). Antigen retrieval was performed by incubating free-floating sections in 10 mM sodium citrate buffer (pH 6.0) at 80 °C for 1 h. Sections were washed in PBS and then were blocked in 5 % normal goat serum in 1xPBS with 0.1 % TritonX-100 for 1 h at room temperature. Sections were then incubated with primary antibodies in blocking buffer overnight at 4 °C. Sections were washed and stained with appropriate fluorescent secondary antibodies in blocking buffer for 1 h at room temperature. After washing and counterstaining with DAPI, sections were mounted on Superfrost Plus slides (Fisher Scientific) and coverslipped with Prolong Gold anti-fade medium (Life Technologies, Eugene, OR). For thioflavin-S (ThioS) staining, adjacent sections to those stained for 6E10 and Iba1 were selected. Unstained sections were mounted on slides prior to staining in 1 % ThioS in ddH_20. ThioS stained slides were counterstained with propidium iodide to stain nuclei, washed in ddH_20 and coverslipped with Permount (Fisher Scientific). All images were taken on a Leica epifluorescent microscope at 5× magnification. Images were analyzed by a blinded observer using Image Pro-Plus software (Media Cybernetics, Silver Spring, MD).

Behavior

Open Field Test (OFT)—OFT was performed to measure activity levels and anxiety-like behavior. Breifly, Mice were removed from their home cage and placed individually in a square open-field with a video camera positioned above. Mice were allowed to freely explore the space for 15 min and then were returned to their home cage. Open-field apparatus was cleaned with 70 % ethanol before and after each mouse to eliminate odor cues. Data were analyzed using Ethovision software (Noldus). Total distance and time spent in the periphery and the center of the field was determined.

Novel Object Recognition (NOR)—To asses cognitive ability, NOR was performed as previously described (Donkin et al. 2010). Briefly, mice were placed in the same open-field with two identical objects for the training phase of NOR. Mice were allowed to freely explore the space and the objects for 10 min. Mice were then returned to their home cage for 3 h. For the testing phase of NOR, mice were returned to the same open-field, with one of the objects they encountered in the training phase (familiar object), and a novel object. Mice were allowed to freely explore the space and objects for 6 min. Time spent investigating each object (t) was determined by manual scoring by a blinded observer using ODlog software (Macropod Software). Mice that investigated for a total of less than 7 s, or only investigated one object, were omitted from analysis (<5 % of mice evaluated). Investigation index was determined by the following equation: $(t_{(novel)} - t_{(familiar)}) / t_{(total)}$ = investigation index.

Fear Conditioning—Fear conditioning was performed as described previously with minor modifications (Cramer et al. 2012). Briefly, experiments were performed using two standard conditioning chambers, each of which was housed in an isolation cubicle and equipped with a stainless-steel grid floor connected to a solid-state shock scrambler. Each scrambler was connected to an electronic constant-current shock source that was controlled via an interface connected to a Windows XP computer running FreezeFrame software (Coulbourn Instruments, Allentown, PA). A digital camera was mounted on the steel ceiling of each chamber, and video signals were sent to the same computer for analysis. During training, mice were placed in the conditioning chamber for 2.5 min and then received one mild footshock (0.4 mA, 2 s), followed by another 2.5 min. Hippocampus-dependent contextual fear memory formation and was evaluated by scoring freezing behavior for 5 min when the mice were placed back into the same conditioning chamber 24 h after training.

qPCR

Quantification of pro- or anti-inflammatory gene expression was performed as previously described (Cameron et al. 2012). Briefly, RNA was isolated from RNA-Bee (Tel-Test) preserved protein homogenate samples using the RNeasy Mini Kit (Qiagen) according to the manufacturer's instructions. RNA samples (0.5 μg) were reverse transcribed using QuantiTect Reverse Transcription kit (Quiagen). cDNA was run in a 10 μL reaction for 40 cycles on the StepOne Plus Real Time PCR system (Applied Biosystems) using the TaqMan Gene Expression Master Mix (Life Technologies). Primers were all TaqMan assays labeled with FAM (Life Technologies) and included Il-1β (Mm01336189_m1), IL6 (Mm00446190_m1), Tnfα (Mm99999068_m1), TGFβ (Mm01178820_m1), CCL2

(Mm00441242_m1), ATF3 (Mm00476032_m1), YM1 (Mm00657889_mH), and GAPD H (4352339E-0904021). The comparative CT method ($\Delta\Delta C_T$) was used to normalize Ct values to internal control (GAPDH) and analyze gene expression. Statistics were performed at the ΔC_T level (prior to exponential transformation). For ease of interpretation, results are expressed in fold change from ABCA1 WT – Veh group. Graphs represent the average fold change (RQ)±RQ min and max for each group.

Statistical Analysis

All graphs are represented as the mean of each group±SEM. Data was analyzed by two way ANOVA followed by Bonferroni post-hoc tests, or select paired t-tests, as indicated. Results were considered statistically significant when p-values were less 0.05. All statistical analysis was performed using GraphPad Prism 5 software.

Results

Bexarotene-Induced Upregulation of Lipidated ApoE Requires ABCA1

We hypothesize that the mechanism of action of bexarotene in the clearance of soluble Aβ relies on the lipidation status of ApoE (Cramer et al. 2012). Western blot analysis of the HP and CX revealed that bexarotene caused a significant upregulation of proteins associated with reverse cholesterol transport, ABCA1 and ApoE, in ABCA1 WT mice (Fig. 1). As expected, ABCA1 protein was undetectable in the HP or CX of ABCA1 KO mice (Fig. 1b, d). ABCA1 KO mice exhibited a 50 % reduction in ApoE levels compared with ABCA1 WT mice in the CX ($F(1,48)=48.23$, $p<0.0001$) and HP ($F(1,44)= 168.1$, $p<0.0001$), and these ApoE levels were not increased by bexarotene treatment (Fig. 1c, e. In contrast, ApoE levels were significantly increased by bexarotene treatment in ABCA1 WT mice. There was a significant interaction between ABCA1 genotype and bexarotene treatment in the CX ($F(1,48)=8.636$, $p<0.01$) and HP ($F(1,48)=9.209$, $p<0.01$), indicating that ABCA1 was required for the bexarotene-mediated upregulation of ApoE.

Because the ability of ApoE to mediate Aβ clearance is dependent on lipidation status (Jiang et al. 2008), ApoE HDL levels in CX and HP homogenates were also measured. Native gel analysis, which resolved ApoE-based HDLs by size, revealed a bexarotene-mediated increase in highly lipidated ApoE in ABCA1 WT mice (Fig. 2). ABCA1 deficiency was associated with a significant decrease in lipidated ApoE in the CX ($F(1,48)=261.8$, $p<0.0001$) and HP ($F(1,48)=124.4$, $p<0.0001$), and bexarotene treatment caused no changes in lipidated ApoE in the CX or HP of ABCA1 KO mice (Fig. 2b, c). In addition, there was a significant interaction between ABCA1 genotype and bexarotene treatment in the CX ($F(1,48)=14.51$, $p<0.001$) and HP ($F(1,48)=12.32$, $p<0.001$), indicating that ABCA1 is necessary for the bexarotene to increase levels of highly-lipidated ApoE.

Bexarotene-Induced Decrease in Hippocampal Levels of Soluble Aβ 40 and 42 Requires ABCA1

We next determined if the inability of ABCA1 KO mice to increase lipidation of ApoE would alter the ability of bexarotene to clear soluble and insoluble Aβ from the CX and HP. We isolated DEA and FA soluble fractions of CX and HP homogenates to analyze the

soluble and insoluble fractions of Aβ, respectively. We found that soluble levels of Aβ 40 and 42 were significantly reduced in the HP of ABCA1 WT mice after bexarotene treatment, but not in ABCA1 KO mice (Fig. 3a, b). Insoluble levels of Aβ 40 and 42 in the HP were unaffected by bexarotene treatment (Fig. 3c, d). These data indicate that bexarotene caused a reduction in hippocampal levels of soluble Aβ that was dependent on functional ABCA1.

In contrast with the HP, there were no bexarotene-induced changes in soluble or insoluble levels of Aβ 40 or 42 in the CX regardless of ABCA1 genotype (data not shown). Although, soluble levels of Aβ 40 were increased in the CX of ABCA1 KO mice compared with ABCA1 WT (data not shown). These data indicate that bexarotene may have region specific effects in various mouse models, consistent with previous reports (Riddell et al. 2007).

Deficiency of ABCA1 was associated with increased soluble and insoluble Aβ pathology, as has been shown previously (Koldamova et al. 2005; Wahrle et al. 2005). ABCA1 KO mice showed an increase in soluble Aβ40 ($F(1,48)=21.39$, $p<0.0001$), but not soluble Aβ 42, when compared with ABCA1 WT mice (Fig. 3a, b). Levels of insoluble Aβ 40 ($F(1,48)=6.844$; $p<0.05$) and Aβ 42 ($F(1,48)=14.92$, $p<0.001$) were increased in ABCA1 KO mice (Fig. 3c, d).

ABCA1 Deficiency Causes an Increase in Plaque Pathology and Activated Microglial Morphology

Because we saw an increase in insoluble Aβ 40 and 42 in the HP of ABCA1 KO mice we hypothesized that this increase would be associated with increased plaque pathology in ABCA1 KO mice. In addition, it was possible that reduced soluble Aβ in the HP of bexarotene treated ABCA1 WT mice would be associated with decreased plaque pathology. To further investigate the ABCA1-dependent effects of bexarotene treatment on Aβ pathology, we used an immunohistochemical approach. Free-floating coronal brain sections (25 μm) were costained with antibodies to Aβ (6E10) and Iba1 to analyze diffuse and dense-core plaque pathology and microglial phenotype, respectively. ABCA1 KO mice showed increases in levels of 6E10 immunoreactivity and Iba1, compared with ABCA1 WT mice (Fig. 4). For example, there were significant differences in plaque area in the CX between ABCA1 WT vehicle-treated mice and ABCA1 KO treated mice (Fig. 4c; $p<0.05$) and between ABCA1 WT bexarotene-treated mice and ABCA1 KO vehicle-treated mice (Fig. 4e; $p<0.05$). Similar trends in iba1 immunoreactivity were observed in ABCA1 KO mice in the CX and HP (Fig. 4d, f). To better visualize microglial morphology, a higher magnification image taken from the boxed region in Fig. 1a shows a marked increase in activated microglial morphology in the ABCA1 KO mice (Fig. 1gi and ii). These results indicate that ABCA1 KO mice show increased plaque pathology that is associated with increased abundance of microglia with an activated morphology. Bexarotene did not significantly alter plaque pathology in ABCA1 WT mice, as evaluated by 6E10 staining. (Fig. 4c, e).

To determine if dense-core plaques were affected by bexarotene treatment, we stained brain sections with ThioS and analyzed the area occupied by dense-core plaques. ABCA1 WT mice showed no change in dense-core plaque pathology, while ABCA1 KO mice showed a trend towards a bexarotene-induced decrease (Fig. 5). These results verify that the role of

bexarotene-stimulated amyloid clearance is due principally to the action of ABCA1 in promoting degradation of soluble Aβ forms rather than plaques.

ABCA1 is Necessary for Bexarotene-Induced Improvement in Novel Object Recognition

Because of the well-known link between changes in soluble Aβ and cognitive function (Palop and Mucke 2010), we hypothesized that the decreased HP levels of Aβ 40 and 42 in the ABCA1 WT mice following bexarotene treatment would be associated with improved cognitive performance. In the novel object recognition (NOR) test, we found a pronounced deficit in both ABCA1 WT ($p=0.099$) and KO ($p<0.05$) mice bred on an APP/PS1 background, compared with non-transgenic controls (Fig. 6a). Following bexarotene treatment, ABCA1 WT mice showed a trend towards improved recognition of the novel object ($p=0.11$), but this effect was absent in ABCA1 KO mice (Fig. 6a). This effect was not associated with reduced locomotion or increased anxiety, as measure by the open field activity test (data not shown), indicating that bexarotene improved cognitive ability in ABCA1 WT mice without causing changes in baseline behavior. These data indicate that ABCA1 is necessary for bexarotene to improve cognitive ability in the novel object recognition test.

Contextual fear conditioning was also tested. ABCA1 WT mice bred on an APP/PS1 background showed significantly impaired fear memory compared to non-transgenic controls, however, bexarotene did not improve this deficit (Fig. 6b). In contrast, ABCA1 KO mice bred on an APP/PS1 background did not show a deficit in fear memory compared with nontransgenic controls and did not show a change in behavior after bexarotene treatment.

ABCA1 Deficiency is Associated with Altered Inflammatory Gene Expression

Thus far, we have determined that ABCA1 is necessary for bexarotene to induce a reduction in soluble Aβ from the HP and this reduction is associated with improved cognitive ability. These data support our hypothesis that bexarotene requires ABCA1-mediated ApoE lipidation for soluble Aβ clearance. We have also hypothesized that bexarotene may affect microglial inflammation states independently of functional ABCA1. Importantly, it is known that HDL is an important mediator of inflammation in the brain (Hottman et al. 2014). Previous studies have found that ABCA1-deficient mice exhibit increased levels of inflammation (Karasinska et al. 2013). It is possible that bexarotene may cause different inflammatory profiles in the absence of ABCA1. To explore this hypothesis, we isolated total RNA from the CX and HP and performed qPCR on a panel of inflammatory genes. The genes examined included classic proinflammatory cytokines, IL-1β, IL-6, and TNFα. The anti-inflammatory cytokine, TGFβ was examined because of its known involvement with AD pathology (Town et al. 2008). The proinflammatory chemokine CCL2 was examined as a marker of inflammation and because of the potential role of peripheral macrophage recruitment (El Khoury et al. 2007). ATF3 was also examined because of its role as a transcription factor that is controlled by HDL and is a master regulator of inflammation (De Nardo et al. 2014). As expected, both ABCA1 WT and KO mice on an APP/PS1 background had higher levels of inflammatory gene expression when compared to non-transgenic controls (Fig. 7) (Mandrekar-Colucci et al. 2012). For example in 2 way ANOVA

analysis, a main effect of APP/PS1 genotype was found for every gene examined in the HP and CX, indicating an enhanced inflammatory environment in APP/PS1 mice.

ABCA1 KO genotype was associated with higher levels of inflammation. Two way ANOVA analysis was performed to determine the effects and interactions of ABCA1 genotype and bexarotene treatment in APP/PS1 mice. Figure 7a shows that ABCA1 KO mice had higher levels of TNFα, CCL2, and TGFβ expression in the CX compared with ABCA1 WT mice (TNFα $F(1,33)=50.43$, $p<0.0001$; CCL2 $F(1,33)=9.552$, $p<0.01$; TGFβ $F(1,33)=20.15$, $p<0.0001$). In the HP, similar trends were observed (Fig. 7b). For example HP expression levels of TNFα and YM1 were increased in ABCA1 KO mice compared with ABCA1 WT mice (TNFα $F(1,32)=4.197$, $p<0.05$; YM-1 $F(1,32)=12.99$, $p<0.001$). Interestingly, we observed almost no difference in inflammatory gene expression between non-transgenic ABCA1 WT and non-transgenic ABCA1 KO control mice. The only exception was a significant increase in IL-1β expression in the HP of non-transgenic ABCA1 KO mice compared with non-transgenic ABCA1 WT mice ($p<0.01$). These data indicate that ABCA1 deficiency leads to an enhanced inflammatory environment in the context of APP/PS1 background.

Bexarotene treatment in both ABCA1 WT and KO mice caused increased levels of most inflammatory genes in the CX, including IL-6, TGFβ, CCL2, and ATF3 (IL-6, $F(1,33)=8.913$, $p<0.01$; TGFβ, $F(1,33)=19.44$, $p<0.0001$; CCL2, $F(1,33)=17.23$, $p<0.001$; ATF3 $F(1,33)=8.623$, p,0.01). Similar results were found the HP, where IL-6 and TGFβ were significantly increased by bexarotene treatment (IL-6, $F(1,33)=13.53$, $p<0.001$; TGFβ, $F(1,33)=6.882$, $p<0.05$). In all genes where bexarotene induced an increase in inflammatory gene expression, there was no interaction between bexarotene and ABCA1. This indicates that although ABCA1 KO mice had higher inflammatory gene expression in general, bexarotene induced a similar effect in both ABCA1 WT and ABCA1 KO mice. Notably, the only gene where there was an interaction between ABCA1 genotype and bexarotene treatment was in IL-1β. In the CX, IL-1β was decreased by bexarotene treatment in ABCA1 KO mice, but not in ABCA1 WT mice (CX, $F(1,33)=12.10$, $p<0.01$). In the HP, this effect was present but was not statistically significant (HP, $F(1,33)=3.704$, $p=0.06$). With the exception of IL-1β, bexarotene induced an increased expression of inflammatory markers regardless of ABCA1 deficiency, indicating that the inflammatory effects of bexarotene are likely not essential for the mechanism of action of soluble Aβ clearance.

Discussion

Our data support the hypothesis that ABCA1 is necessary for the primary action of bexarotene in clearing soluble Aβ. We showed that ABCA1 is necessary for bexarotene to increase ApoE expression, and its lipidation (Figs. 1 and 2). ABCA1 WT mice showed a ~30 % decrease in soluble levels of Aβ40 and 42 in the HP following bexarotene treatment, which was absent in the ABCA1 KO mice (Fig. 3). Furthermore, decreased levels of soluble Aβ in the HP were associated with improved cognitive ability in the novel object recognition test (Fig. 6). It has been previously shown that ABCA1 is necessary for the LXR agonist, GW3965, to reduce Aβ pathology and reverse deficits in novel object recognition (Donkin et al. 2010). The present data are consistent with this previous finding. Taken together, the

results of the current study show that ABCA1 is necessary for the RXR agonist, bexarotene, to clear soluble Aβ and improve cognitive ability in a mouse model of AD.

Previous studies have shown ABCA1 activity to be a potent modulator of Aβ pathophysiology in several mouse models of AD. The current study confirms and extends these previous findings. For example, consistent with previous studies (Hirsch-Reinshagen et al. 2005; Koldamova et al. 2005; Wahrle et al. 2005), we found increased soluble and insoluble levels of Aβ, along with increased plaque pathology. It is likely that ABCA1 deficiency is at least a partial cause of the increased Aβ pathology in ABCA1 KO mice, because genetic overexpression of ABCA1 caused an opposing effect, with a pronounced reduction in levels of soluble Aβ and plaques (Wahrle et al. 2008). In agreement with previous papers, we show that ABCA1 KO mice have a reduction in brain ApoE levels (Hirsch-Reinshagen et al. 2004; Wahrle et al. 2004), and ApoE could not be induced by bexarotene in ABCA1 KO mice (Figs. 1 and 2). Because bexarotene is believed to act at the gene expression level (Skerrett et al. 2014), the lack of effect of bexarotene on ApoE expression in ABCA1-deficient mice is not immediately intuitive. This apparent conflict is likely caused by the instability of poorly-lipidated ApoE in ABCA1 KO mice, leading to increased catabolism, rather than reduced Apoe gene expression (Hirsch-Reinshagen et al. 2004; Wahrle et al. 2004). In mouse models of AD crossed with ABCA1 KO mice, higher levels of insoluble ApoE were found co-deposited with Aβ, indicating that poorly lipidated ApoE may exacerbate Aβ pathology (Hirsch-Reinshagen et al. 2005). The findings of this study support the important role of ABCA1-mediated ApoE lipidation in AD pathophysiology.

Bexarotene treatment induced a marked decrease in soluble Aβ in the hippocampus, but this effect was not associated with decreased insoluble Aβ levels, or decreased plaque pathology (6E10 or ThioS staining; Figs. 4 and 5). Although some studies have shown that bexarotene treatment was able to clear plaque deposition (Cramer et al. 2012; Savage et al. 2015) the present findings are consistent with other studies where bexarotene induced a reduction in levels of soluble, but not insoluble or deposited, Aβ in mouse models of AD (Castellano et al. 2011; Fitz et al. 2013; Price et al. 2013; Tesseur et al. 2013; Veeraraghavalu et al. 2013). Indeed, we reported that the effect of bexarotene varies with age, the animal model, and duration of treatment (Cramer et al. 2012). The reasons for inconsistent findings regarding the ability of bexarotene to clear plaque pathology are unknown. However, plaque pathology is generally a poor indicator of cognitive function in human AD patients and in animal models (Landreth et al. 2013). However, in other studies of bexarotene where plaque deposition was not observed, a bexarotene-induced benefit in cognition was still present (Fitz et al. 2013; Tesseur et al. 2013). Here we show that reduced levels of soluble Aβ 40 and 42 in the hippocampus were associated with a trend towards improved performance in the novel object recognition test. We interpret these data to indicate that bexarotene may affect cognition primarily by clearing soluble Aβ rather than insoluble Aβ and plaques.

In this study, we found that there were brain region-specific effects of bexarotene. Specifically, we found a bexarotene-induced decrease of soluble Aβ in the HP but not in the CX. This result is similar to a previous study using the LXR agonist, TO901317, where hippocampal levels of Aβ42 were reduced but there was no change in cortical Aβ following

LXR agonist treatment (Riddell et al. 2007). It is unknown why the effects of nuclear receptor agonists on pathology would be region specific. Although, brain region specific effects have been linked to relative levels of Aβ pathology in another study where an AD mouse model was treated with bexarotene (Tai et al. 2014). Specifically, bexarotene was found to reduce levels of Aβ 42 in the HP, but not the CX, of an AD mouse model expressing human ApoE4 (Tai et al. 2014). Thus, the hippocampus may be more susceptible to the Aβ-clearing effects of nuclear receptor agonists, and this fact may contribute to improved hippocampal-dependent cognitive ability following treatment.

In addition to stimulating reverse cholesterol transport and increased levels of lipidated ApoE, nuclear receptor agonists influence the neuroinflammatory environment of the brain (Zelcer et al. 2007). In addition it is known that HDL is an important mediator of inflammation in the brain (Hottman et al. 2014). In this study we found that bexarotene caused an increase in most inflammatory markers, regardless of ABCA1 genotype. The effect of bexarotene on inflammation in AD models has not previously been examined and the basis of this paradoxical effect is unexplained. It is unknown how bexarotene may be altering inflammation since RXRs are not found at the corepressor complex of the NFκB promoter, but it is possible that ligation of RXR influences the actions of its heterdimeric partner including LXRs and PPARs (Saijo et al. 2013). An alternative notion, is that microglia may not be directly involved with clearance of soluble or insoluble Aβ, as depletion of microglia from the normal mouse brain with a CSF1R antagonist (PLX3397) resulted in little effect on behavior or cognition, despite inflammatory changes (Elmore et al. 2014). These findings indicate that altered inflammatory profiles following bexarotene treatment is not an essential component of soluble Aβ clearance.

The inflammatory effects of ABCA1 deficiency have not been studied extensively. We found that ABCA1 KO mice had increased gene expression levels of several inflammatory markers, including TNFα, TGFβ, and CCL2. This exaggerated neuroinflammatory phenotype in ABCA1 KO mice on an APP/PS1 background was associated in this study with increased Iba1 expression, indicating that a more reactive microglial phenotype may underlie this effect. There was no effect of ABCA1-deficiency on neuroinflammatory phenotype in non-AD model mice, however, indicating that impaired ABCA1 activity may predispose microglia to increased inflammation in the context of AD or another inflammatory stimulus. In support of this notion, mice with ABCA1 deficiency specifically in brain (ABCA1$^{-B/-B}$ mice) had increased cortical expression of TNFα, TGFβ, and INOS, and increased MAPK signaling following peripheral LPS injection (Karasinska et al. 2013). Thus, ABCA1 deficiency may pre-dispose the brain to an exaggerated inflammatory response. Exaggerated inflammation in ABCA1 KO mice may depend on other factors, such as ApoE genotype. For example, ABCA1 hemizygosity had a detrimental effect in ApoE4 targeted replacement mice, but had no effect on pathology in ApoE3 targeted replacement mice on an APP/PS1 background (Fitz et al. 2012). We interpret these data to indicate that altered inflammatory activity in the ABCA1-deficient mice likely contributes to exaggerated Aβ pathology.

Based on this study and previous work, we propose that lipidated ApoE is an important factor in the clearance of soluble Aβ. We show here that ABCA1-mediated lipidation of

ApoE was a necessary factor for the mechanism of action of bexarotene. Nuclear receptor agonists represent a useful tool for studying the mechanisms of Aβ clearance from the brain. RXR agonists, such as bexarotene, are generally well-tolerated, but are not without side effects. An alternative approach would be to increase ABCA1 expression through a direct transcriptional approach. For example, a recent study used an miR-33 anti-sense oligonucleotide to increase ABCA1 at the transcriptional level (Jan et al. 2015). In conclusion, this study lends support to the role of ABCA1-mediated lipidation of ApoE in the clearance of soluble Aβ, and improvement of cognitive deficits in an AD mouse model.

References

Bateman RJ, Munsell LY, Morris JC, Swarm R, Yarasheski KE, Holtzman DM (2006) Human amyloid-beta synthesis and clearance rates as measured in cerebrospinal fluid in vivo. Nat Med 12:856–861 [PubMed: 16799555]

Cameron B, Tse W, Lamb R, Li X, Lamb BT, Landreth GE (2012) Loss of interleukin receptor-associated kinase 4 signaling suppresses amyloid pathology and alters microglial phenotype in a mouse model of Alzheimer's disease. J Neurosci: OFF J Soc Neurosci 32:15112– 15123

Castellano JM, Kim J, Stewart FR, Jiang H, DeMattos RB, Patterson BW, Fagan AM, Morris JC, Mawuenyega KG, Cruchaga C, Goate AM, Bales KR, Paul SM, Bateman RJ, Holtzman DM (2011) Human apoE isoforms differentially regulate brain amyloid-beta peptide clearance. Sci Transl Med 3:89ra57

Cramer PE, Cirrito JR, Wesson DW, Lee CY, Karlo JC, Zinn AE, Casali BT, Restivo JL, Goebel WD, James MJ, Brunden KR, Wilson DA, Landreth GE (2012) "ApoE-directed therapeutics rapidly clear beta-amyloid and reverse deficits in AD mouse models". Science 335: 1503–1506 [PubMed: 22323736]

De Nardo D, Labzin LI, Kono H, Seki R, Schmidt SV, Beyer M, Xu D, Zimmer S, Lahrmann C, Schildberg FA, Vogelhuber J, Kraut M, Ulas T, Kerksiek A, Krebs W, Bode N, Grebe A, Fitzgerald ML, Hernandez NJ, Williams BR, Knolle P, Kneilling M, Rocken M, Lutjohann D, Wright SD, Schultze JL, Latz E (2014) High-density lipoprotein mediates anti-inflammatory reprogramming of macrophages via the transcriptional regulator ATF3. Nat Immunol 15: 152–160 [PubMed: 24317040]

Donkin JJ, Stukas S, Hirsch-Reinshagen V, Namjoshi D, Wilkinson A, May S, Chan J, Fan J, Collins J, Wellington CL (2010) ATP-binding cassette transporter A1 mediates the beneficial effects of the liver X receptor agonist GW3965 on object recognition memory and amyloid burden in amyloid precursor protein/presenilin 1 mice. J Biol Chem 285:34144–34154 [PubMed: 20739291]

El Khoury J, Toft M, Hickman SE, Means TK, Terada K, Geula C, Luster AD (2007) Ccr2 deficiency impairs microglial accumulation and accelerates progression of Alzheimer-like disease. Nat Med 13:432–438 [PubMed: 17351623]

Elmore MR, Najafi AR, Koike MA, Dagher NN, Spangenberg EE, Rice RA, Kitazawa M, Matusow B, Nguyen H, West BL, Green KN (2014) Colony-stimulating factor 1 receptor signaling is necessary for microglia viability, unmasking a microglia progenitor cell in the adult brain. Neuron 82:380–397 [PubMed: 24742461]

Fitz NF, Cronican AA, Saleem M, Fauq AH, Chapman R, Lefterov I, Koldamova R (2012) Abca1 deficiency affects Alzheimer's disease-like phenotype in human ApoE4 but not in ApoE3-targeted replacement mice. J Neurosci: OFF J Soc Neurosci 32:13125–13136

Fitz NF, Cronican AA, Lefterov I, Koldamova R (2013) Comment on "ApoE-directed therapeutics rapidly clear beta-amyloid and reverse deficits in AD mouse models". Science 340:924–c

Hirsch-Reinshagen V, Zhou S, Burgess BL, Bernier L, McIsaac SA, Chan JY, Tansley GH, Cohn JS, Hayden MR, Wellington CL (2004) Deficiency of ABCA1 impairs apolipoprotein E metabolism in brain. J Biol chem 279:41197–41207 [PubMed: 15269218]

Hirsch-Reinshagen V, Maia LF, Burgess BL, Blain JF, Naus KE, McIsaac SA, Parkinson PF, Chan JY, Tansley GH, Hayden MR, Poirier J, Van Nostrand W, Wellington CL (2005) The absence of

ABCA1 decreases soluble ApoE levels but does not diminish amyloid deposition in two murine models of Alzheimer disease. J Biol Chem 280: 43243–43256 [PubMed: 16207707]

Hottman DA, Chernick D, Cheng S, Wang Z, Li L (2014) HDL and cognition in neurodegenerative disorders. Neurobiol Dis 72(Pt A):22–36 [PubMed: 25131449]

Jan A, Karasinska JM, Kang MH, de Haan W, Ruddle P, Kaur A, Connolly C, Leavitt BR, Sorensen PH, Hayden MR (2015) Direct intracerebral delivery of a miR-33 antisense oligonucelotide into mouse brain increases brain ABCA1 expression. Neurosci Lett 598:66–72 [PubMed: 25957561]

Jankowsky JL, Slunt HH, Ratovitski T, Jenkins NA, Copeland NG, Borchelt DR (2001) Co-expression of multiple transgenes in mouse CNS: a comparison of strategies. Biomol Eng 17:157–165 [PubMed: 11337275]

Jiang Q, Lee CY, Mandrekar S, Wilkinson B, Cramer P, Zelcer N, Mann K, Lamb B, Willson TM, Collins JL, Richardson JC, Smith JD, Comery TA, Riddell D, Holtzman DM, Tontonoz P, Landreth GE (2008) ApoE promotes the proteolytic degradation of Abeta. Neuron 58:681–693 [PubMed: 18549781]

Karasinska JM, de Haan W, Franciosi S, Ruddle P, Fan J, Kruit JK, Stukas S, Lutjohann D, Gutmann DH, Wellington CL, Hayden MR (2013) ABCA1 influences neuroinflammation and neuronal death. Neurobiol Dis 54:445–455 [PubMed: 23376685]

Koldamova R, Staufenbiel M, Lefterov I (2005) Lack of ABCA1 considerably decreases brain ApoE level and increases amyloid deposition in APP23 mice. J Biol Chem 280:43224–43235 [PubMed: 16207713]

Koldamova R, Fitz NF, Lefterov I (2010) The role of ATP-binding cassette transporter A1 in Alzheimer's disease and neurodegeneration. Biochim Biophys Acta 1801:824–830 [PubMed: 20188211]

Landreth GE, Cramer PE, Lakner MM, Cirrito JR, Wesson DW, Brunden KR, Wilson DA (2013) Response to comments on "ApoE-directed therapeutics rapidly clear beta-amyloid and reverse deficits in AD mouse models". Science 340:924–g

Mandrekar-Colucci S, Karlo JC, Landreth GE (2012) Mechanisms underlying the rapid peroxisome proliferator-activated receptor-gamma-mediated amyloid clearance and reversal of cognitive deficits in a murine model of Alzheimer's disease. J Neurosci Off J Soc Neurosci 32:10117–10128

Palop JJ, Mucke L (2010) Amyloid-beta-induced neuronal dysfunction in Alzheimer's disease: from synapses toward neural networks. Nat Neurosci 13:812–818 [PubMed: 20581818]

Price AR, Xu G, Siemienski ZB, Smithson LA, Borchelt DR, Golde TE, Felsenstein KM (2013) Comment on BApoE-directed therapeutics rapidly clear beta-amyloid and reverse deficits in AD mouse models. Science 340:924–d

Riddell DR, Zhou H, Comery TA, Kouranova E, Lo CF, Warwick HK, Ring RH, Kirksey Y, Aschmies S, Xu J, Kubek K, Hirst WD, Gonzales C, Chen Y, Murphy E, Leonard S, Vasylyev D, Oganesian A, Martone RL, Pangalos MN, Reinhart PH, Jacobsen JS (2007) The LXR agonist TO901317 selectively lowers hippo-campal Abeta42 and improves memory in the Tg2576 mouse model of Alzheimer's disease. Mol Cell Neurosci 34:621–628 [PubMed: 17336088]

Saijo K, Crotti A, Glass CK (2013) Regulation of microglia activation and deactivation by nuclear receptors. Glia 61:104–111 [PubMed: 22987512]

Savage JC, Jay T, Goduni E, Quigley C, Mariani MM, Malm T, Ransohoff RM, Lamb BT, Landreth GE (2015) Nuclear receptors license phagocytosis by trem2+ myeloid cells in mouse models of Alzheimer's disease. J Neurosci: OFF J Soc Neurosci 35:6532–6543

Skerrett R, Malm T, Landreth G (2014) Nuclear receptors in neurodegenerative diseases. Neurobiol Dis 72(Pt A):104–116 [PubMed: 24874548]

Tai LM, Koster KP, Luo J, Lee SH, Wang YT, Collins NC, Ben Aissa M, Thatcher GR, LaDu MJ (2014) Amyloid-beta Pathology and APOE Genotype Modulate Retinoid X Receptor Agonist Activity in Vivo. J Biol Chem 289:30538–30555 [PubMed: 25217640]

Tesseur I, Lo AC, Roberfroid A, Dietvorst S, Van Broeck B, Borgers M, Gijsen H, Moechars D, Mercken M, Kemp J, D'Hooge R, De Strooper B (2013) Comment on BApoE-directed therapeutics rapidly clear beta-amyloid and reverse deficits in AD mouse models. Science 340:924–e

Town T, Laouar Y, Pittenger C, Mori T, Szekely CA, Tan J, Duman RS, Flavell RA (2008) Blocking TGF-beta-Smad2/3 innate immune signaling mitigates Alzheimer-like pathology. Nat Med 14:681–687 [PubMed: 18516051]

Veeraraghavalu K, Zhang C, Miller S, Hefendehl JK, Rajapaksha TW, Ulrich J, Jucker M, Holtzman DM, Tanzi RE, Vassar R, Sisodia SS (2013) Comment on BApoE-directed therapeutics rapidly clear beta-amyloid and reverse deficits in AD mouse models. Science 340: 924–f

Verghese PB, Castellano JM, Holtzman DM (2011) Apolipoprotein E in Alzheimer's disease and other neurological disorders. Lancet Neurol 10:241–252 [PubMed: 21349439]

Wahrle SE, Jiang H, Parsadanian M, Legleiter J, Han X, Fryer JD, Kowalewski T, Holtzman DM (2004) ABCA1 is required for normal central nervous system ApoE levels and for lipidation of astrocyte-secreted apoE. J Biol Chem 279:40987–40993 [PubMed: 15269217]

Wahrle SE, Jiang H, Parsadanian M, Hartman RE, Bales KR, Paul SM, Holtzman DM (2005) Deletion of Abca1 increases Abeta deposition in the PDAPP transgenic mouse model of Alzheimer disease. J Biol Chem 280:43236–43242 [PubMed: 16207708]

Wahrle SE, Jiang H, Parsadanian M, Kim J, Li A, Knoten A, Jain S, Hirsch-Reinshagen V, Wellington CL, Bales KR, Paul SM, Holtzman DM (2008) Overexpression of ABCA1 reduces amyloid deposition in the PDAPP mouse model of Alzheimer disease. J Clin Invest 118:671–682 [PubMed: 18202749]

Wildsmith KR, Holley M, Savage JC, Skerrett R, Landreth GE (2013) Evidence for impaired amyloid beta clearance in Alzheimer's disease. Alzheimers Res Ther 5:33 [PubMed: 23849219]

Zelcer N, Khanlou N, Clare R, Jiang Q, Reed-Geaghan EG, Landreth GE, Vinters HV, Tontonoz P (2007) Attenuation of neuroinflammation and Alzheimer's disease pathology by liver x receptors. Proc Natl Acad Sci U S A 104:10601–10606 [PubMed: 17563384]

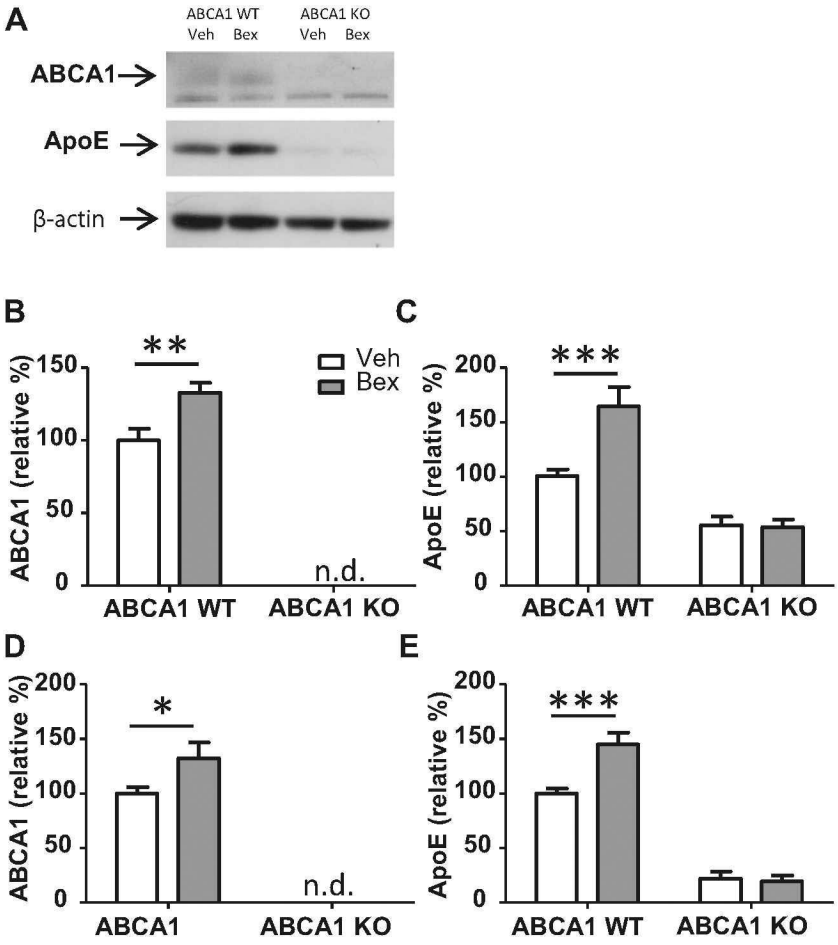

Fig. 1.

Bexarotene-induced upregulation of ABCA1 and ApoE requires ABCA1. ABCA1 WT and KO mice were crossed with APP/PS1 mice (females; 10 months). Mice were treated with bexarotene (100 mg/kg/day p.o.) or vehicle for 7 days. Following drug treatment, mice were sacrificed and cortex and hippocampus (CX and HP) were dissected separately from the right hemisphere of the brain. Brain regions were homogenized and western blotting analysis was performed for ABCA1, ApoE, and β-actin. **a** A representative blot is shown from CX samples. Quantification of western blots are shown in **b**, **c** for CX samples and **d**, **e** for HP samples. Bands were normalized to β-actin to ensure equal loading, and then expressed as a relative percentage of ABCA1 WT vehicle-treated mice. Bars represent the mean± SEM of each group (n=10–12). 2 way ANOVA analysis with Bonferroni posttest was performed. * $p<0.05$, ** $p<0.01$, ***$p<0.001$

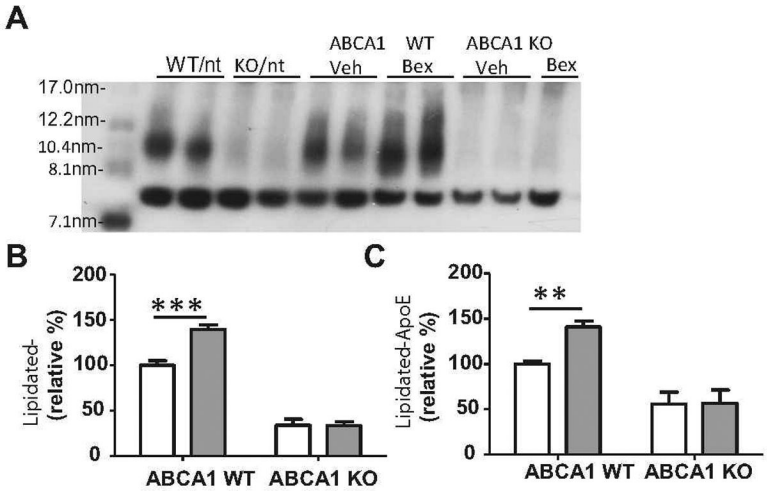

Fig. 2.

Bexarotene-induced increase in lipidated ApoE requires ABCA1. ABCA1 WT and KO mice were crossed with APP/PS1 mice (females; 10 months). Mice were treated with bexarotene (100 mg/kg/day p.o.) or vehicle for 7 days. Following drug treatment, mice were sacrificed and cortex and hippocampus (CX and HP) were dissected separately from the right hemisphere of the brain. Brain regions were homogenized and native western blots were perfomed under non-denaturing conditions. a representative blot is shown for CX samples with standard molecular weight marker in far left lane. Quantification of western blots are shown for b CX and c HP. Bands are expressed as a relative percentage of ABCA1 WT vehicle-treated mice. Bars represent the mean±SEM of each group (n=10–12). 2 way ANOVA analysis with Bonferroni posttest was performed. ** $p<0.01$, *** $p<0.001$

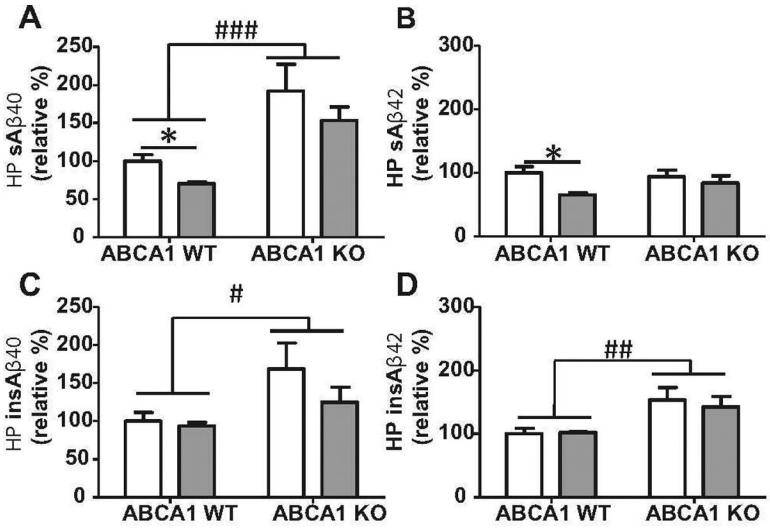

Fig. 3.

Bexarotene-induced decrease in HP levels of soluble Aβ 40 and 42 requires ABCA1. ABCA1 WT and KO mice were crossed with APP/ PS1 mice (females; 10 months). Mice were treated with bexarotene (100 mg/kg/day p.o.) or vehicle for 7 days. Following drug treatment, mice were sacrificed and hippocampus (HP) was dissected from the right hemisphere of the brain. HP was homogenized and levels of soluble and insoluble Aβ40 and 42 were measured by ELISA. **a** and **b** show levels of soluble Aβ40 and 42, respectively. **c** and **d** show levels of insoluble Aβ40 and 42, respectively. Bars represent the mean ± SEM of each group expressed as a relative percent of ABCA1 WT vehicle-treated mice (n=10–12). Two way ANOVA analysis with Bonferroni posttest was performed. # indicates significant main effect of ABCA1 genotype, # $p<0.05$, ## $p<0.01$, ### $p<0.001$. * indicates significant difference in Bonferonni post-hoc test, * $p<0.05$

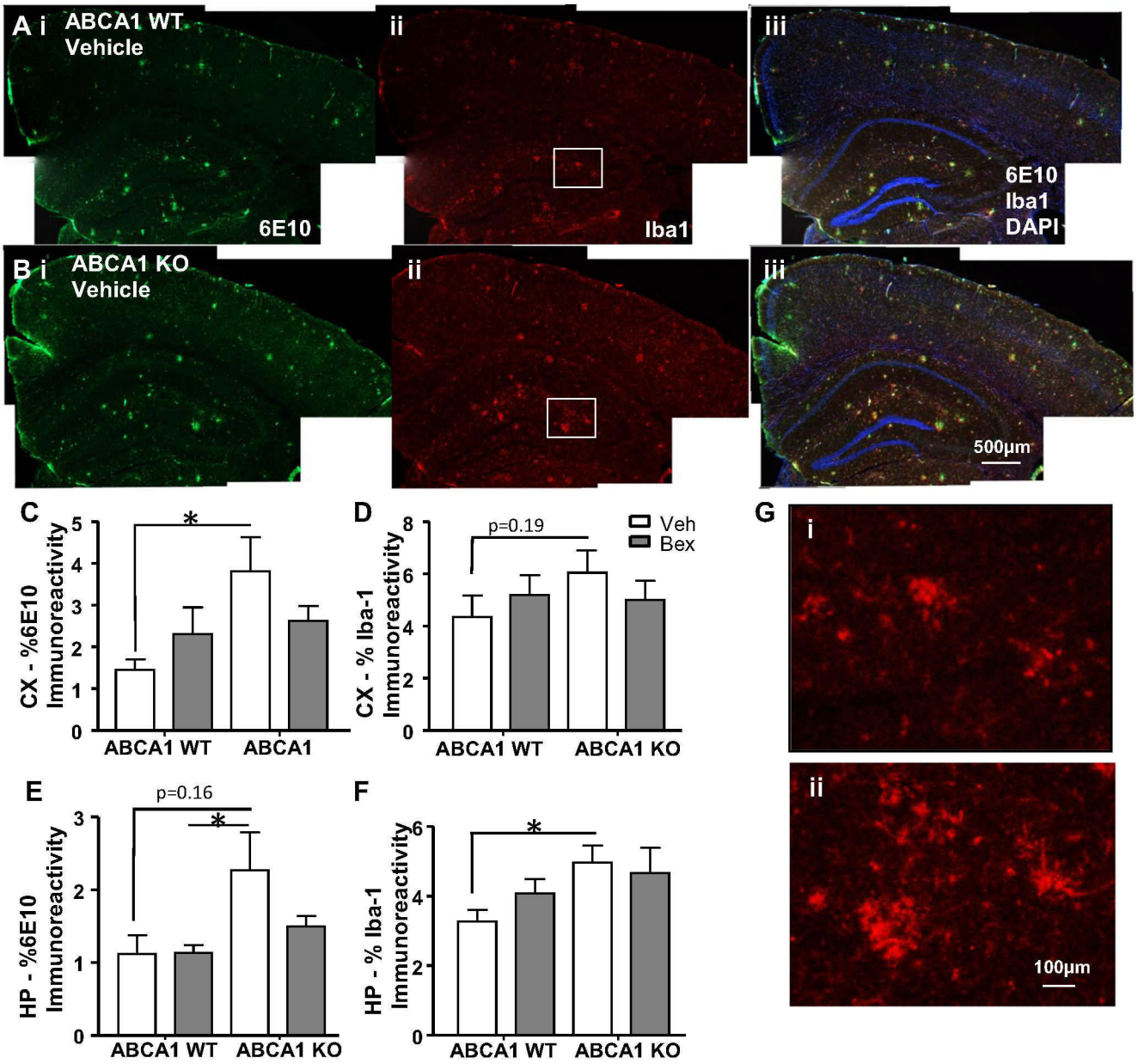

Fig. 4.

ABCA1 deficiency causes an increase in plaque pathology and activated microglial morphology. ABCA1 WT and KO mice were crossed with APP/PS1 mice (females; 10 months). Mice were treated with bexarotene (100 mg/kg/day p.o.) or vehicle for 7 days. After sacrifice, brains were processed for 6E10 and Iba1 immunostaining. **a**-**b**) Representative staining for ABCA1 WT and ABCA1 KO vehicle-treated mice is shown. Staining for CX and HP is quantified in **c**-**f**. **g** Higher magnification image of iba1 staining from boxed region in i Aii, and ii Bii. Bars represent the mean±SEM of each group (n=10–12). Select two tailed unpaired t-tests were performed. * $p<0.05$

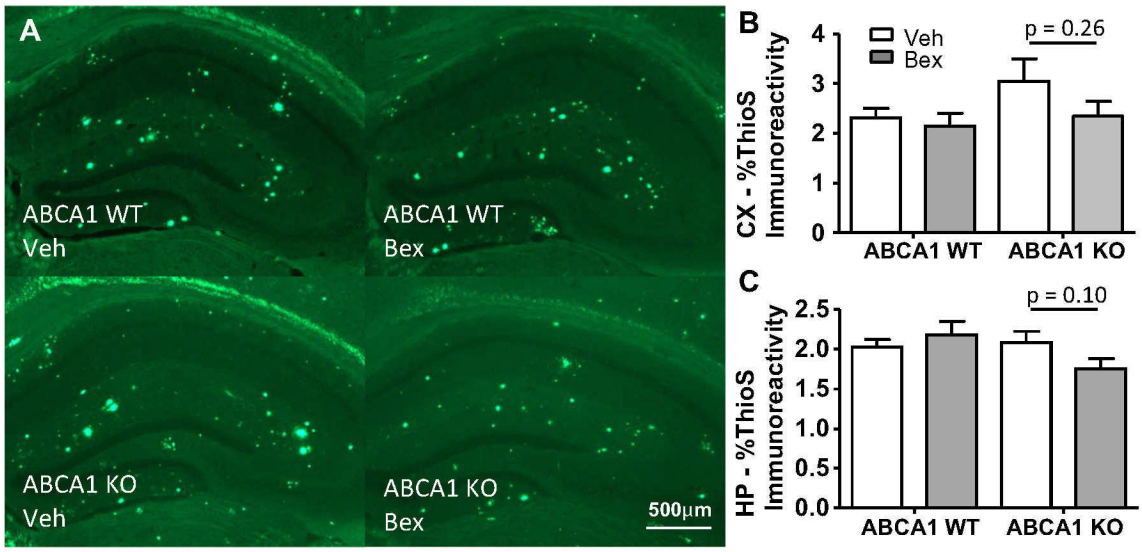

Fig. 5.

Dense-core plaque pathology was unaltered by bexarotene treatment. ABCA1 WT and KO mice were crossed with APP/PS1 mice (females; 10 months). Mice were treated with bexarotene (100 mg/kg/day p.o.) or vehicle for 7 days. After sacrifice, brains sections were stained for ThioS. **a** Representative staining of HP. Staining for CX and HP is quantified in **b** and **c**, respectively. Bars represent the mean±SEM of each group (n=10–12). Select two tailed unpaired t-tests were performed. * $p<0.05$

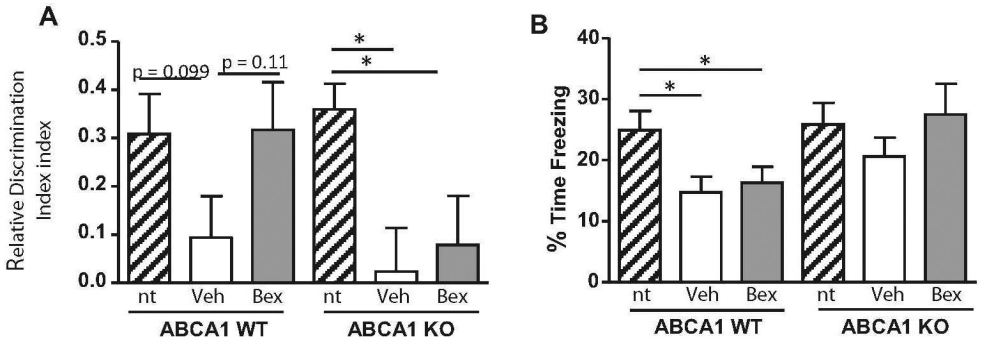

Fig. 6.

ABCA1 is necessary for bexarotene-induced improvement in novel object recognition. ABCA1 WT and KO mice were crossed with APP/PS1 or non-transgenic (nt) mice (females; 10 months). Mice were treated with bexarotene (100 mg/kg/day p.o.) or vehicle for 7 days. Prior to sacrifice, mice were tested for **a** novel object recognition (NOR) ability, and **b** memory in fear conditioning test. Bars represent the mean±SEM of each group (n=10–12). One way ANOVA was performed. * $p<0.05$

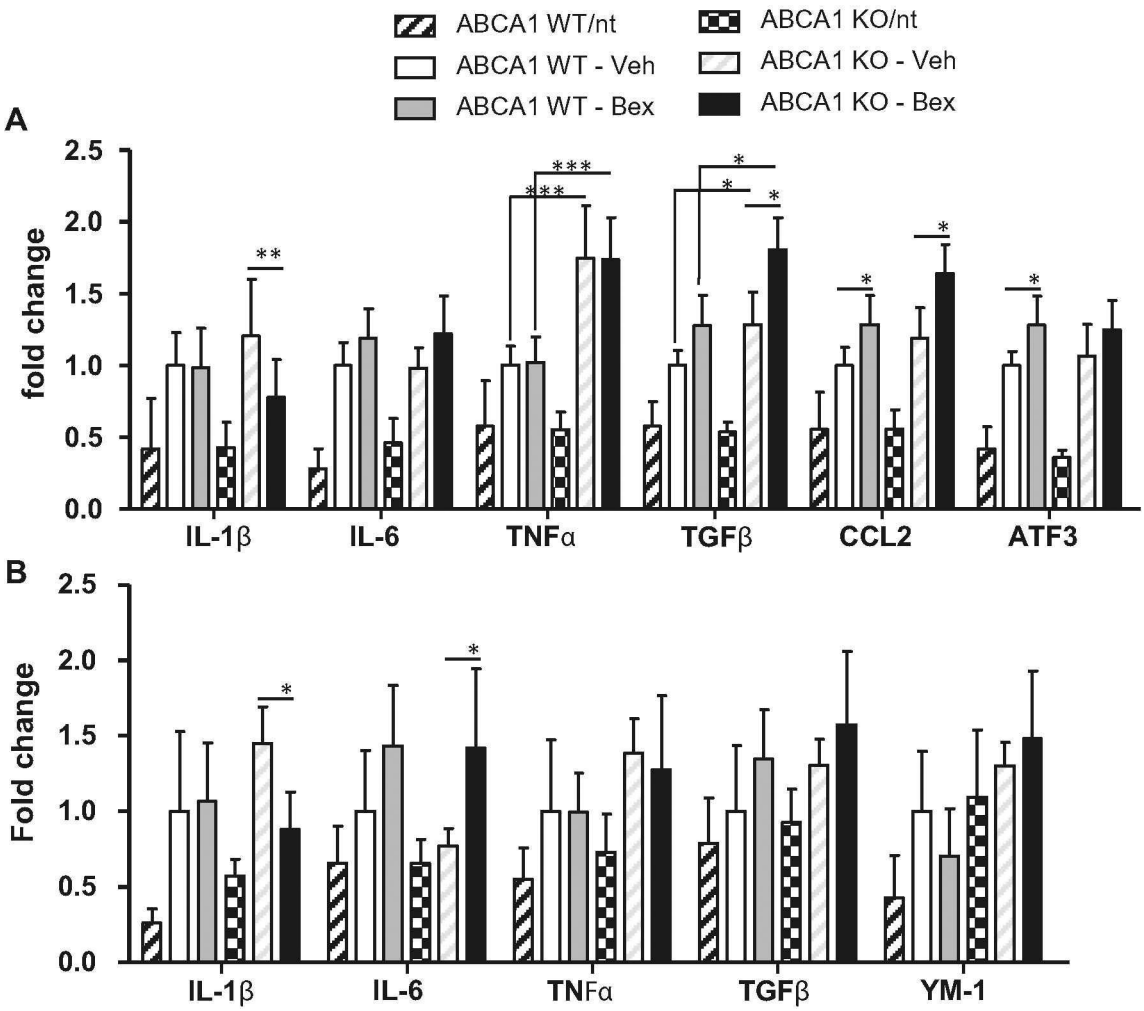

Fig. 7.

ABCA1 KO mice show increased inflammatory markers at baseline and bexarotene treatment increases inflammatory markers. ABCA1 WT and KO mice were crossed with APP/PS1 or nontransgenic (nt) mice (females; 10 months). Mice were treated with bexarotene (100 mg/kg/day p.o.) or vehicle for 7 days. Total RNA was isolated from the **a** CX and B) HP and qPCR for the indicated genes was performed. Results are expressed in fold change from ABCA1 WT – Veh group. Bars represent the average fold change (RQ) ± RQ min and max of each group (n=10–12). One-way ANOVA was performed. For ease of interpretation, only significant interactions between ABCA1 WT-Veh vs. ABCA1 WT-Bex, ABCA1 KO-Veh vs ABCA1 KO-Bex, ABCA1 WTVeh vs. ABCA1 KO-Veh, and ABCA1 WT-Bex vs ABCA1 KO Bex, are shown. * $p<0.05$. ** $p<0.01$, ***$p<0.001$